



# In situ LIBS-XRF analysis as a combined approach to disclose the production technology of unique wall mirrors from Pompeii

Iliaria Costantini<sup>1,a</sup> , Marco Veneranda<sup>2</sup>, Nagore Prieto-Taboada<sup>1</sup>, Kepa Castro<sup>1</sup>, Silvia Fdez-Ortiz de Vallejuelo<sup>1</sup>, Idoia Etxebarria Román<sup>1</sup>, Bruno de Nigris<sup>3</sup>, Alberta Martellone<sup>3</sup>, Juan Manuel Madariaga<sup>1,4</sup>, Gorka Arana<sup>1</sup>

<sup>1</sup> Department of Analytical Chemistry, Faculty of Science and Technology, University of the Basque Country (UPV/EHU), 48080 Bilbao, Spain

<sup>2</sup> Department of Condensed Matter Physics, Crystallography and Mineralogy, University of Valladolid (UVa), Valladolid, Spain

<sup>3</sup> Archaeological Park of Pompeii, Via Villa Dei Misteri 2, 80045 Pompei Scavi, Pompei, Italy

<sup>4</sup> Unesco Chair of Cultural Landscapes and Heritage, University of the Basque Country (UPV/EHU), Vitoria-Gasteiz, Spain

Received: 17 October 2022 / Accepted: 22 June 2023

© The Author(s) 2023

**Abstract** It is assumed that the unique wall mirrors found at the Archaeological Park of Pompeii (PAP) are made of obsidian. To contribute to the knowledge of those archaeological artefacts, this work proposes *in situ* elemental analyses in collaboration with PAP seeking to determine, in a total non-destructive way, the composition and provenance of the main mirror preserved at the House of Gilded Cupids. Comparing the geochemical composition of this black glass with that of obsidian samples collected from the main Mediterranean sources, both X-ray fluorescence (XRF) and laser-induced breakdown spectroscopy (LIBS) confirmed an incompatible content of many key elements. LIBS in-depth analysis excluded the potential relation between the higher concentration of Ca and Mg and the presence of alteration products. In addition, XRF analysis missed the detection of Rb, Y, Zr and Nb, which are widely recognized as the elemental fingerprints of obsidian sources. Combined with the detection of a high content of strontium (500–700 ppm), the *in situ* elemental data proved that, rather than made of obsidian, the analysed mirror was handcrafted by the fusion of coastal sand. Waiting to extend this study to the other mirrors found at Pompeii, the results here presented indicate the history of these unique artefacts needs to be rewritten.

## 1 Introduction

The eruption of Mount Vesuvius that occurred in 79 AD buried the city of Pompeii under several meters of volcanic ashes, pumices and debris [1]. The volcanic material sealed the remains of the Roman city, favouring its optimal preservation until modern days. Beyond the world famous wall paintings [2, 3] and mosaics [4, 5] decorating Pompeian residences and public buildings, the archaeological excavations started in the eighteenth century (and still ongoing) enabled the retrieval of many daily life objects that contributed to unveil new information about Roman habits and customs. Among them, the wall mirrors decorating the House of Gilded Cupids (two mirrors), the Domus of Euplia (one) and the House of Efebo (one) represent a particularly interesting case of study [6]. Indeed, to the authors' knowledge, these are only artefacts of this kind to be ever retrieved from Roman archaeological sites.

Due to their vitreous composition, black colour, and shiny appearance, Pompeian mirrors have always been considered to be made of obsidian. Indeed, being a very resistant volcanic glass formed by rapidly cooled lava [7], obsidian has been widely employed since prehistoric age to craft numerous kinds of weapons, tools and ornamental objects [8]. Knowing that 1) the number of obsidian sources exploited and/or commercialized under the Roman empire were quite limited, and 2) each obsidian outcrop presents an unique and very homogeneous chemical composition (data dispersion estimated in  $\pm 1\%$  for major elements and between 2 and 5% for minor and trace elements [9]), geochemical analysis can be used to disclose the provenance of ancient obsidian artefacts [10, 11]. Inductively coupled plasma mass spectrometry (ICP-MS) [12, 13], particle-induced X-ray emission (PIXE) [10, 14], scanning electron microscope (SEM) [15] and X-ray fluorescence (XRF) [16, 17] benchtop instruments have been widely used for this purpose, providing excellent results. By comparing the elemental composition of archaeological artefacts with obsidian fragments sampled from the main Mediterranean sources, geochemical analyses can be effectively used to determine the provenance of obsidian objects, thus reconstructing ancient trading routes [8].

Although the mentioned analytical methods could effectively indicate composition and origin of raw materials, the common assumption that Pompeian wall mirrors are made of obsidian has only recently been reconsidered [18]. On the one hand, this is due to the fact that sampling the glass material is strictly forbidden, which makes impossible to carry out laboratory analyses. On the other hand, despite the good results so far provided by portable XRF instruments [11, 19–21], the reliability of *in situ* provenance

<sup>a</sup> e-mail: [iliana.costantini@ehu.eus](mailto:iliana.costantini@ehu.eus) (corresponding author)

methods applied to the study of highly degraded or altered artefacts (as is the case of Pompeian wall mirrors) still needs to be assessed.

In a previous study, carried out by the IBeA Research group through the in situ use of portable spectroscopic techniques, the conservation of the two mirrors found at the House of the Gilded Cupids was proved to be threatened by the deposition of nitrates, sulphates and goethite crusts [6]. Caused by the impact of atmospheric acid pollutants such as CO<sub>2</sub>, NO<sub>x</sub> and SO<sub>x</sub>, the elemental composition of these alteration products could affect in situ XRF analysis, compromising the reliability of provenance studies.

To overcome that issue, the development of a dedicated method to discriminate the nature of Pompeian wall mirrors was established as one of the main aims of the scientific collaboration between the Archaeological Park of Pompeii (PAP) and IBeA. Working in this research line the research group recently published a novel method for in situ discrimination of Mediterranean obsidian sources [22]. Based on the combined use of portable XRF and LIBS systems [23], the discrimination method proved the in situ characterization of degraded obsidian artefacts can be optimized by taking advantage of the complementarity between both spectroscopic techniques [24]. On the one hand, in-depth LIBS analyses allow to determine whether the concentration of K, Ca, Mg and Al (as major components of obsidians) is affected by the presence of superficial alteration products. On the other hand, XRF analyses carried out using specific fundamental parameter methods optimize the detection of Rb, Sr, Y, Zr and Nb [25], which are widely known as the elemental fingerprints for obsidian sources [21].

Continuing with our research program, a new analysis campaign was carried out to gather all the elemental data necessary to disclose the nature of the major wall mirror found at the House of Gilded Cupids. Thus, in situ XRF and LIBS analyses were carried out by setting the same analytical parameters employed in the previous optimization work [22]. Afterwards, in situ results were compared to those provided by reference samples to investigate whether obsidian was effectively employed as raw material. Based on the results derived from the application of the tailored provenance method, the geochemistry of the wall mirror was further compared to those of additional vitreous artefacts to discern the real origin of the raw material used to produce the Pompeian wall mirror found in the House of Gilded Cupids.

## 2 Materials and methods

### 2.1 Wall mirrors from the house of gilded cupids

The IBeA research group (University of the Basque Country UPV/EHU) has a long collaboration history with PAP. Since 2014, the scientific partnership has been mainly focused on the in situ study of the House of Gilded Cupids. Located at the Regio IV, Insula 16.7, this residence was built in the first century, and it was named after the gilded plates (decorated with cupids' figures) that were retrieved from the house. Once owned by Cn. Poppaeus Habitus (related to Poppea Sabina, Nerone's second wife), the House of the Gilded Cupids stands out by the extraordinary richness and variety of its archaeological remains. Besides frescoes, fountains, polychrome mosaics, marble sculptures and Roman and Egyptians lalariums [26], the east wall of the peristyle is enriched by the presence of two wall mirrors. As represented in Fig. 1, the first mirror has a rhomboid shape and a size of 35 × 20 cm, while the second has an irregular shape and a size of 20 × 15 cm. Together with those recovered from the House of Efebo (I 7, 10–12.19) and the Domus of Euplia (I 9, 5–7), they represent the only wall mirrors found so far at this archaeological site [6].

### 2.2 Obsidian reference samples

Starting from the widely held assumption that Pompeian wall mirrors were made of volcanic glass, a multi-analytical research work was recently carried out to estimate the capability of the portable XRF and LIBS instruments described in Sect. 2.4 to discriminate Mediterranean obsidian sources [22]. For this purpose, the elemental composition of obsidian samples collected from Lipari [27], Palmarola [28], Pantelleria [29] and Sardinia [30] (SA, SB1, SB2 and SC varieties) was investigated.

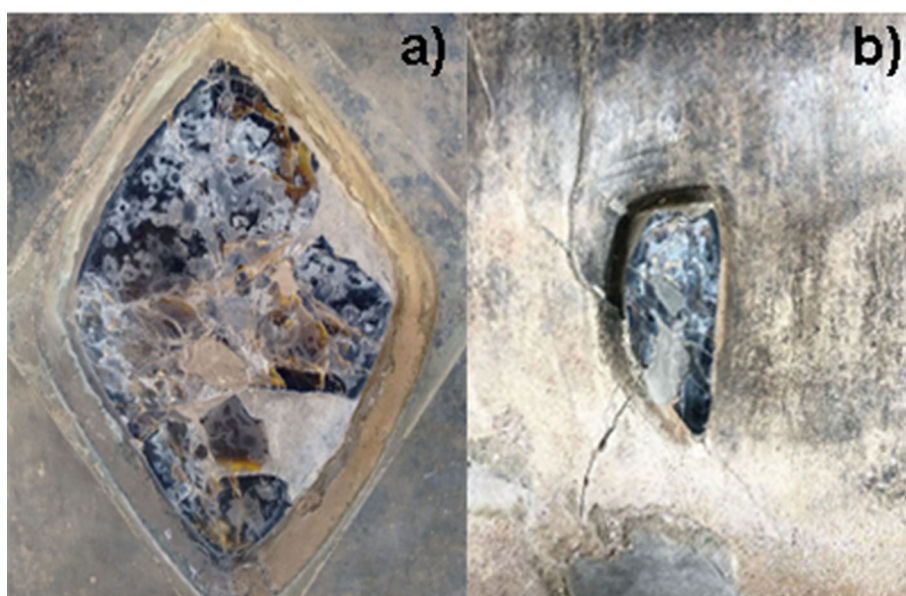
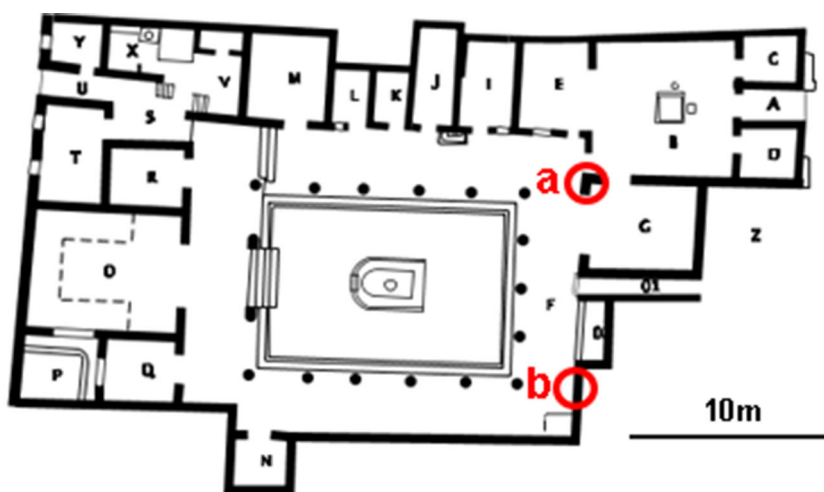
The results obtained in the previous work proved the suitability of both elemental techniques for obsidian sourcing [31–33]. Besides demonstrating the perfect complementarity between LIBS and XRF systems, our work enabled to identify, for each spectroscopic technique, the elemental parameters optimizing obsidian's discrimination. As such, the elemental parameters and the PCA-based discrimination models presented in the manuscript were used in the present work to verify whether the wall mirror was effectively made of obsidian and identify the corresponding Mediterranean source.

### 2.3 Analytical techniques

The research here presented was focused on the use of portable XRF and LIBS systems, which reliability for materials classification has been confirmed in previous works [34, 35].

XRF analyses were carried out through a handheld XMET5100 spectrometer (Oxford Instruments, Oxford UK) equipped with a rhodium anode X-ray tube and a silicon drift detector having energy and resolutions of 150 eV and 20 eV, respectively. As detailed elsewhere [25], this instrument's software allows the selection of different analytical methods, which can be used to adjust the elemental detection to the composition of the analysed target. In this study, each spot of interest (with a diameter of 9 mm) was

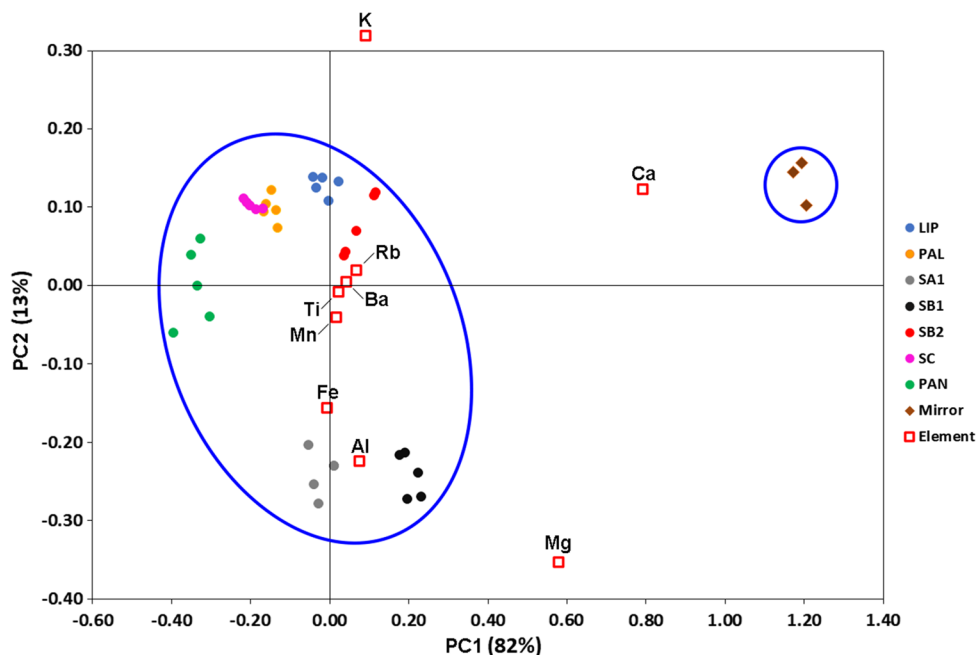
**Fig. 1** Floor plan of the House of the Golden Cupids, combined with the image of the two mirrors located at the east wall of the peristyle



investigated using both SoilFP and SoilLEFP methods. (Further information is provided in Sect. 3.2.) Regarding obsidian standards, 5 points per sample were analysed. On the other side, the main mirror preserved at the House of Gilded cupids was analysed at 7 different spots that, according to in situ microscopic observations and molecular spectroscopic analysis presented in a previous work [6], did not show any detectable alteration feature. In both cases, spectra were acquired during 100 s (real time) to improve the limit of detection for the identification of trace elements.

In situ LIBS spectra were acquired using the EasyLIBS commercial system (IVEA, model Easy 2C). This instrument is equipped with a pulsed Nd:YAG laser, emitting at 1064 nm. The laser beam is focused by a 15-cm focal-length converging lens, which produces a spot of analysis of around 500  $\mu\text{m}$  in diameter. The plasma signal is finally collected by three spectrometers, covering the ultraviolet (UV, 196–419 nm), the visible (VIS, 420–579 nm) and the near-infrared (NIR, 580–1000 nm) spectral ranges (HR2000 + /Ocean Optics, USA) with a resolution of 0.2 nm. In this work, measurements were taken with the double pulse mode by setting an optimized delay time of 50  $\mu\text{s}$  to the laser pulse and a gate width of 5 ms. The laser energy per pulse on the sample was set to 30 mJ with a repetition rate of 1 Hz and a duration of 5 ns. For each obsidian sample, 5 spectra were collected by accumulating 20 laser-shots from the same spot of analysis. Considering the micro-invasiveness of this analytical technique, the number of analyses performed on the Pompeian mirror was reduced to three spots. In this case of study, 20 laser shots were accumulated from each spot. By taking advantage of the camera coupled to the system, the laser beam was focused on areas that were completely free of any form of visible alterations. The AnaLIBS 6.3 software was used for automatic spectra acquisition and visualization, while peaks identification was carried out using the NIST database [36].

**Fig. 2** Scores and loadings plots from the PCA of LIBS data. K variable has been represented outside the graph, as its PC2 value is out of scale (0.93)



## 2.4 Data treatment

The SpectPro software [37] was used to visualize, normalize, and compare both LIBS and XRF spectra. Afterwards, the intensity value of the main peak identifying each detected element was calculated using a dedicated MATLAB routine [38]. Agreeing with previous works [31], the characteristic emission lines selected for LIBS were found at 250.1 (Si), 257.5 (Mn), 276.5 (Fe), 279.6 (Mg), 334.9 (Ti), 393.2 (Ca), 396.0 (Al), 455.5 (Ba), 779.8 (Rb), and 766.6 (K). Regarding XRF data, the normalized intensity of  $K\alpha$  peaks found at 1.49 (Al), 1.74 (Si), 3.31 (K), 3.69 (Ca), 4.51 (Ti), 5.90 (Mn), 6.40 (Fe), 8.63 (Zn), 13.40 (Rb), 14.17 (Sr), 14.96 (Y), 15.76 (Zr) and 16.16 (Nb) keV was analysed. To perform the principal components analysis (PCA) of LIBS and XRF data, The Unscrambler®7.6 software (CAMO Software, Oslo, Norway) was used [39]. The normalized intensities of the selected LIBS and XRF peaks were used to fill the data matrix for PCA, which was performed using 6 principal component and cross-validation. Regarding XRF results, additional comparisons have been performed by taking into account the elemental semi-quantitative values provided by the instrument and based on the use of the fundamental parameter (FP) method [40].

## 3 Results

As stated before, in situ analyses based on the combined use of portable XRF and LIBS system have been recently identified as the ideal analytical procedure to characterize the geochemistry of altered obsidian artefacts and to determine the provenance of the raw material [22]. Starting from the widely accepted assumption that Pompeian wall mirrors are made of obsidian, XRF and LIBS portable instruments were used in situ to analyse the main mirror found at the House of the Gilded Cupids by strictly following the analytical procedure proposed elsewhere [22].

### 3.1 LIBS results

As detailed in Sect. 2.3, three in-depth analyses were performed by accumulating 20 laser shots from each selected point of interest. After spectra averaging, baseline correction and intensity normalization, the intensity values of the characteristic elemental peaks listed in Sect. 2.2 were measured. PCA was then used to compare the obtained values to those measured from Mediterranean obsidian sources.

PCA results underlined a clear separation between Pompeian mirror's data and reference obsidian samples. As shown in the score plot presented in Fig. 2, the first principal component (PC1) explains 82% of the variance. By associating scores position with loadings distribution (red squares), it can be inferred that calcium and magnesium are the elemental variables that contribute the most to the separation of Pompeian data from obsidian patterns.

According to the comparison of the LIBS spectra, the intensity of Ca and Mg peaks from the LIBS analysis of the mirror is much higher than those measured from reference obsidian samples. As such, Fig. 3 shows the variation in Mg and Ca contents by taking into account the intensity ratio of their characteristic emission lines (279.5 and 393.2 nm, respectively) to that of Si (251.0 nm),

**Fig. 3** Plot of Ca/Si and Mg/Si LIBS intensity ratios, gathered from the analysis of both obsidian patterns and Pompeian mirror

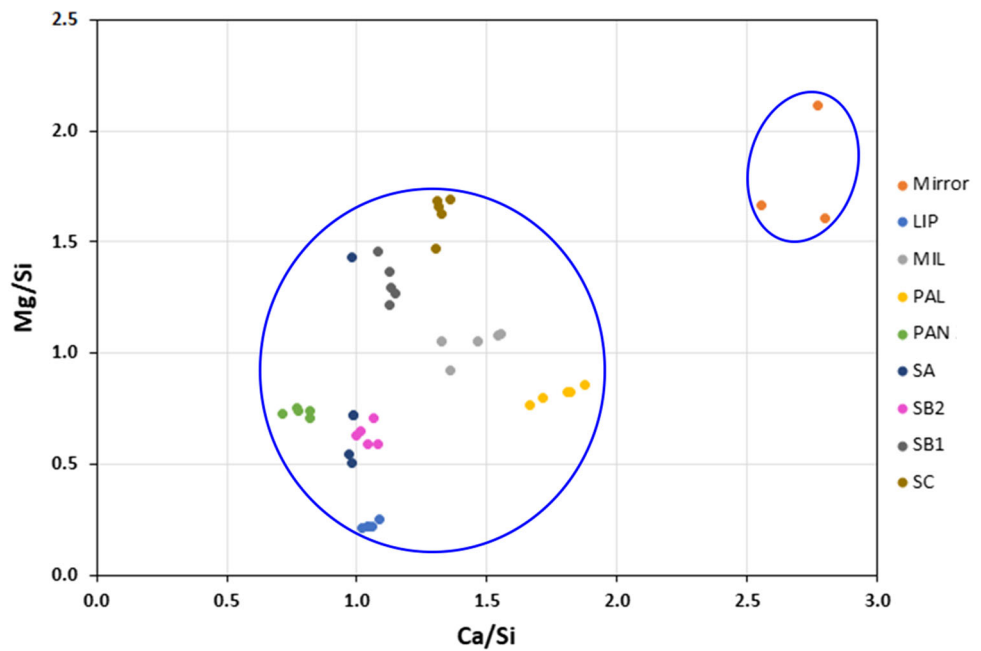


**Table 1** Averaged shots intensity values of Mg and Ca lines at 279.5 and 393.2 nm, respectively

Element	Point of analysis	Averaged intensity			
		Shots 01–05	Shots 06–10	Shots 11–15	Shots 16–20
Mg @ 279.5 nm	Point 1	1.6 ± 0.3	1.7 ± 0.2	1.7 ± 0.2	1.7 ± 0.2
	Point 2	1.5 ± 0.1	1.5 ± 0.1	1.8 ± 0.1	1.6 ± 0.1
	Point 3	2.1 ± 0.4	2.1 ± 0.3	2.3 ± 0.1	2.3 ± 0.4
Ca @ 393.2 nm	Point 1	2.2 ± 0.2	2.7 ± 0.3	2.7 ± 0.2	2.5 ± 0.2
	Point 2	2.3 ± 0.5	2.9 ± 0.3	2.8 ± 0.4	3.0 ± 0.2
	Point 3	2.8 ± 0.4	3.0 ± 0.4	3.0 ± 0.1	2.8 ± 0.1

this being the major component of obsidians (SiO content above 70 wt% depending on the source [41]). The comparison clearly shows that the ratios calculated from mirror’s data are not compatible with those derived from Mediterranean obsidians. In detail, SC (from Monte Arci, Sardinia [42]) is the only obsidian variety displaying Mg/Si ratios (from 1.470 to 1.689) close to mirror’s values (from 1.606 to 2.116). On the contrary, Ca intensity values from Pompeian mirror spectra are far from being compatible with studied obsidian standards, as the calculated Ca/Si ratio (from 2.557 to 2.77) is 73% higher than the closest obsidian reference (Palmarola, from 1.664 to 1.873).

As explained in a previous work [6], the analysed artefact may be affected by the superficial deposition of alteration products, including calcium sulphate (CaSO<sub>4</sub>·2H<sub>2</sub>O), potassium nitrate (KNO<sub>3</sub>) and goethite (FeO(OH)) crusts. As such, the incompatibility between the calculated ratios could be compatible with the presence of micrometric alteration layers (or patina) on the analysed spots, which may have caused a superficial enrichment of Ca and Mg elements.

To evaluate this hypothesis, a pulse-to-pulse spectra comparison was carried out to detect potential elemental fluctuations as moving in depth. Considering the extremely low porosity of obsidians, potential alteration products mostly appear in the form of superficial deposits. In these cases, the relative intensity of Ca and Mg peaks should decrease by increasing the number of LIBS shots, since the material ablation produced by laser pulses would remove the superficial patina. Nevertheless, being Si the main constituent of obsidian glass, its intensity should increase when the number of lasers pulses is sufficient as to penetrate the putative superficial patina and reach the vitreous substrate. Therefore, if superficial depositions of Mg- and Ca-rich alteration products are present, shot after shot, the in-depth LIBS analyses should display a decrease of Mg/Si and Ca/Si ratios.

Considering that each LIBS spectrum was obtained by accumulating 20 laser shots, we compared the Mg/Si and Ca/Si ratios calculated by averaging the intensity values of every 5 consecutive shots. As represented in Table 1, the values obtained by averaging the most superficial shots (1–5) are very similar to those measured from deeper pulses (16–20). Therefore, it can be inferred that the higher content of Ca and Mg is an intrinsic characteristic of the glass geochemistry rather than the result of a superficial elemental enrichment triggered by the putative deposition of micrometric alteration products.

Besides incompatible Mg and Ca contents, LIBS data provided additional analytical information questioning the use of Mediterranean obsidians as raw material. Indeed, it is well known that Mediterranean obsidians present minor contents of Rb, and its

**Fig. 4** Comparison between LIBS spectra gathered from the main Gilded Cupids' mirror (black) and those collected from obsidian standards (red)

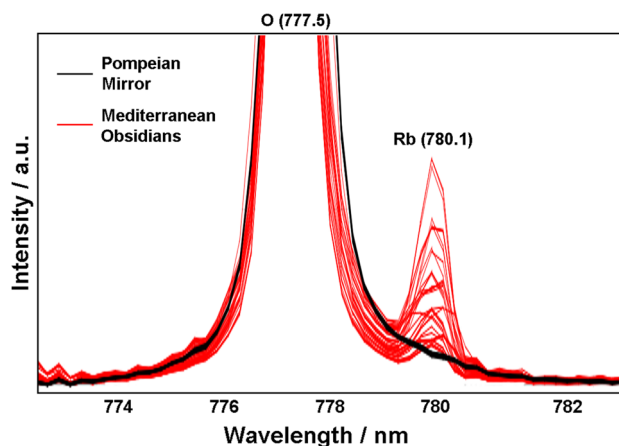
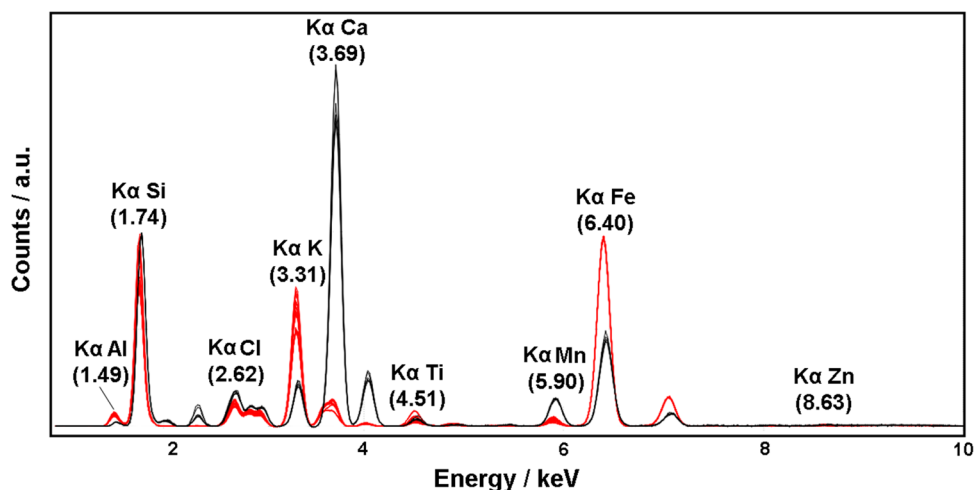


**Fig. 5** Comparison between XRF spectra (SoilLEFP method) gathered from the main Gilded Cupids' mirror (black) with those collected from obsidian patterns (red)



concentration in archaeological artefacts is widely used as elemental fingerprint for provenance studies [43]. As recently presented by Syvilay et al. [31], the same commercial LIBS instrument used in the present work is able to detect Rb traces contained in Mediterranean obsidians. As displayed in the comparison provided in Fig. 4, LIBS spectrum gathered from the main Gilded Cupids' mirror (black lines) does not show any Rb signal, while its characteristic emission line at 780.1 nm was clearly detected in all Mediterranean obsidian (red lines).

Several publications proved that minor amounts of Rb can be detected in all obsidian sources beyond the Mediterranean region [44–47]. As such, the lack of Rb is a strong evidence suggesting that the main Gilded Cupids' mirror was not made of obsidian.

### 3.2 XRF results

Complementary to LIBS investigations, in situ XRF analyses were also carried out. Taking advantage of the non-destructiveness of the technique 7 different areas, considered to be free of macroscopic alteration products, were analysed using two different analytical methods. The SoilLEFP method optimizes the acquisition parameters (voltage of 13 kV and a current of 45  $\mu$ A) to maximize the detection of light elements by focusing the detection of spectral emissions in the range between 0 and 13 keV. On the contrary, the SoilFP method optimizes the detection of the heaviest elements (voltage of 45 kV and a current of 15  $\mu$ A) and extends the analysed spectral range up to 40 keV [25].

When comparing SoilLEFP spectra from the main Gilded Cupids' mirror (Fig. 5, black) with obsidian standards (Fig. 5, red), remarkable differences in the intensity of numerous emissions peaks were detected. Agreeing with LIBS result, the XRF analysis of Pompeian mirrors identified remarkable contents of Ca (3.69 keV), Mn (5.90 keV) and Cl (2.62 keV). In contrast, the detected peaks of K (3.31 keV) and Fe (6.40 keV) are less intense than those gathered from obsidian standards.

As the software controlling the spectrometer calculates, for each analysis, the estimated concentration values of all detected elements, the values expressing Ca, Fe and K contents were represented in a 3D plot. Although the semi-quantitative data gathered by the FP method provide a wide margin of uncertainty, the 3D plot displayed in Fig. 6 clearly shows Gilded Cupids mirror's values do not fit with any obsidian standards. This fact could be interpreted as an additional clue confirming that, despite the starting assumption, the Gilded Cupids mirror was not crafted using obsidian as raw material.

**Fig. 6** 3D plot of Fe, K, and Ca semi-quantitative values obtained from the XRF analysis (SoilLEFP method) of the Gilded Cupids mirror and the obsidian standards

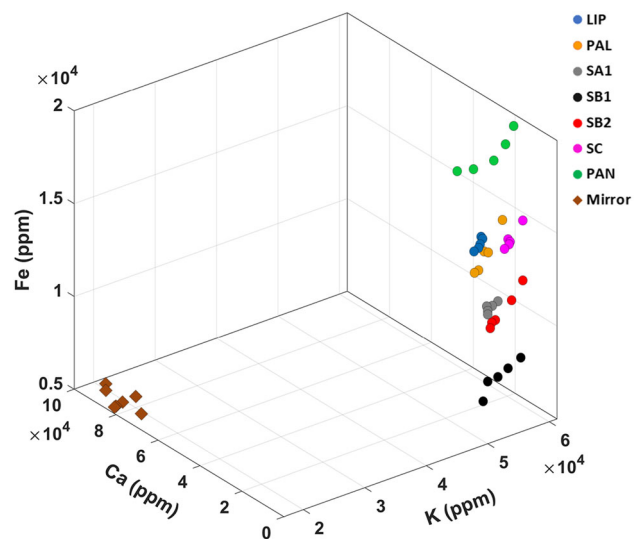
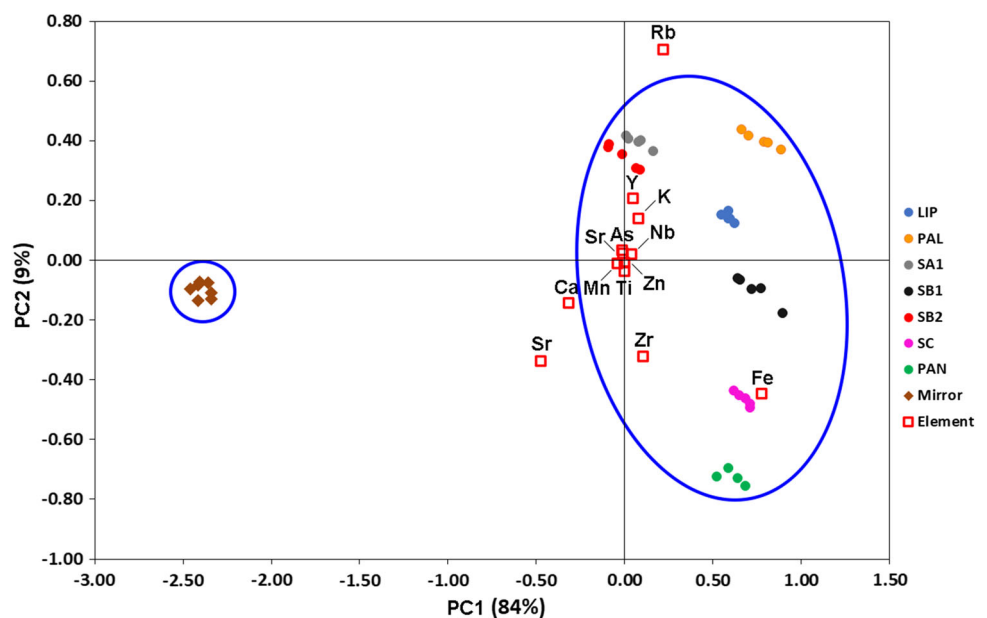


**Fig. 7** Scores and loading plots from the PCA of XRF data (SoilFP method). The K variable has been represented outside the graph, as its PC2 value is out of scale (0.93)



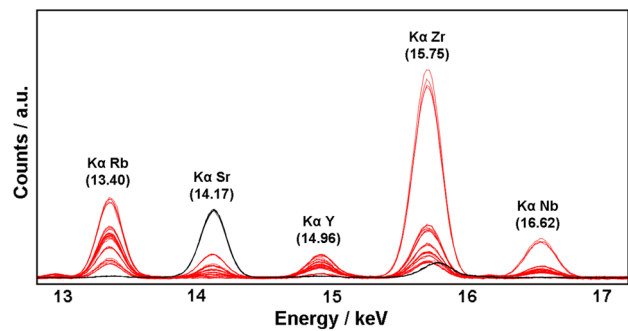
As the detection of the elemental fingerprints is optimized for obsidian sources (Rb, Sr, Y, Zr and Nb) [22], SoilFP XRF data were used to carry out a spectral comparison based on PCA. To do so, the normalized intensity values of the characteristic elemental peaks detected in all spectra were calculated using a dedicated MATLAB routine. Afterwards, PCA of the obtained data matrix was carried out using The Unscrambler software.

PCA results underlined once again a clear separation between the main Gilded Cupids’ mirror and obsidian standards. As displayed in Fig. 7, obsidian sources are mostly resolved through the PC2 axis (explaining 9% of the variance), being Rb, Sr, Zr and Fe the key loadings for their separation. On the other hand, PC1 explains 84% of the variance where the greatest differences between mirror and obsidian data projections lie. By associating scores position with loadings distribution (red squares), it can be inferred that Sr, Ca, Zr, Rb and Fe are the elemental variables that contribute the most to the separation of Gilded Cupids’ mirror data from obsidian standards.

As the PCA results confirmed the key role of some metals in samples discrimination, Fig. 8 compares Gilded Cupids’ mirror and obsidian spectra in the region between 13 and 17 keV. Here, all Mediterranean obsidians (red lines) display different contents of Rb (13.4 keV), Sr (14.2 keV), Y (14.96 keV), Zr (15.78 keV) and Nb (16.62 keV), while the main Gilded Cupids’ mirror (black line) almost completely lacks of Rb, Y and Nb (below 50 ppm).

In addition to that, the FP semi-quantitative values clearly indicate the Gilded Cupids artefact has a much higher content of Sr (between 500 and 700 ppm) compared to obsidian standards (below 200 ppm). As the Pompeian mirror lacks 3 of the 5 elemental

**Fig. 8** Comparison between XRF spectra (SoilFP method) gathered from the main Gilded Cupids' mirror (black) with those collected from obsidian patterns (red)



fingerprints of obsidian sources (while a fourth showed incompatible values), this geochemical study confirmed this artefact is not made of volcanic glass.

Once the use of obsidian was analytically excluded, LIBS and XRF data were used to corroborate the putative use of artificial glass. To do so, the elemental results gathered from the study of the main Gilded Cupids' mirror were compared to ICP-MS, SEM and XRF data obtained from the analysis of Roman vitreous artefacts presented in previous works (see below). For instance, the work presented by De Francesco et al. [48] describes remarkable contents of Mn and Cl in samples of Roman natron glass, these being some of the elements that clearly distinguish the composition of Pompeian mirrors from the investigated obsidian standards.

Among the numerous articles published on this subject, Cagno et al. presented the quantitative elemental analysis of a wide collection of glass fragments from the Roman period [49]. According to ICP-MS data, all fragments contain very low amounts of Y (<15 ppm), Nb (<10 ppm) and Rb (<25 ppm), while the Sr content varies between 300 and 500 ppm. Although our FP semi-quantitative results present a high margin of uncertainty, the values extrapolated from the in situ XRF analyses of the main Gilded Cupids' mirror fit quite well with those presented by Cagno et al. [49]. Focusing on archaeological artefacts recovered within the Italian peninsula, a remarkable Sr content (up to 650 ppm) was recently detected on vitreous fragments found at the Archaeological sites of Herculaneum [50] and Pompeii [51].

As Romans mastered the art of glass production and colouring, it must be underlined that archaeological vitreous artefacts often display strong differences in the concentration of Ca (used in the form of oxide or antimoniate compound to produce white glass), Pb (yellow), Cu (green), Co (blue) and Mn (black) depending on their colour [52]. On the contrary, the Sr content does not vary according to the colour of the analysed artefact [49, 51]. This has been widely acknowledged as a proof that strontium was not employed as colorant additive, but rather represents an elemental impurity of the sand used as the raw material for glass production [53].

Starting from the geochemical analysis of vitreous mosaics *tesserae* from Herculaneum, the origin of the raw materials used for their manufacture was recently investigated [50]. According to the presented results, artificial glasses displaying relatively high contents of strontium can be related to the employment of coastal sand. Indeed, it is well known that Romans mastered the production of the so-called natron glass, which was obtained by using sand, sodium carbonate and lime as former, flux and stabilizer, respectively. From the 5th BC to the 9th AD, the most common production technique consisted in mixing natron with coastal sand characterized by a high content of calcareous particles (acting as stabilizer) in the form of crushed shells [54]. Knowing that seawater contain traces of Sr (around 7 ppm), this element partially substitutes for calcium in shells through a bioaccumulation process [50, 55]. For this reason, detecting Sr contents between 300 and 600 ppm in archaeological glasses was found to be a clear indicator of the use of coastal sands [56], as their Sr value is up to three times higher than the concentration measured in artefacts made of limestone-bearing sand (<200 ppm) [56, 57].

In light of the above, this work suggests that the analysed mirror was handcrafted (probably using coastal sand as raw material for the production of natron glass) rather than made of obsidian.

## 4 Conclusions

In this work, a rare wall mirror preserved at the House of Gilded Cupids (Archaeological Park of Pompeii) was investigated to trace back the origin of the glass material used for its production. Starting from the common assumption that Pompeian wall mirrors were made of obsidian, portable LIBS and XRF instrument were used to characterize the geochemistry of the dark glass in a non-destructive way. Elemental results were then compared to those provided by the study of obsidian fragments sampled from the main Mediterranean sources exploited by Romans. Surprisingly, data analysis based on PCA proved the geochemistry of the wall mirror is far from fitting with obsidian standards. In detail, the LIBS technique detected incompatible amounts of Mg and Ca. In-depth analyses, carried out by accumulating 20 laser shots per point, helped demonstrating that the high contents detected in the mirror are linked to the geochemistry of the glass rather than to an elemental enrichment caused by the superficial deposition of alteration products. Besides confirming LIBS results, XRF spectra additionally detected higher concentrations of Fe and K. However, the



strongest discrepancies detected by this instrument were found in the spectral range between 13 and 17 keV. Here, the main Gilded Cupids' mirror displays the near-total absence of Rb, Y and Nb, which are widely acknowledged as elemental fingerprints for obsidian sourcing. On the contrary, the ancient glass displayed higher amounts of strontium (between 500 and 700 ppm). Compared to the results provided in further studies, the elemental composition of the mirror was found to be compatible with the use of handcrafted glass. Indeed, it is well known that natron glass produced by Romans is rich in Sr, as the coastal sand used as former is enriched with strontium (due to a bioaccumulation process).

In conclusion, in situ LIBS and XRF analysis were able to provide a solid answer to the question that title this manuscript. Against all odds and previous assumptions, the main mirror preserved at the House of Gilded Cupids is not made of obsidian. Rather than that, geochemical analyses point towards the use of artificial glass crafted by Romans using coastal sand as raw silica material. This unexpected result underlines the need of extending the study to the remaining Pompeian mirrors, as the story of these unique artefacts probably needs to be rewritten.

**Acknowledgements** The authors would like to thank the direction of the *Archaeological Park of Pompeii*, for providing access to the study of the obsidian mirror. This work has been financially supported by the DEMORA project (Grant No. PID2020-113391GB-I00), funded by the Spanish Agency for Research (through the Spanish Ministry of Science and Innovation, MICINN, and the European Regional Development Fund, FEDER). I. Costantini acknowledges her postdoctoral contract from the UPV/EHU.

**Funding** Open Access funding provided thanks to the CRUE-CSIC agreement with Springer Nature.

**Data Availability Statement** All data generated or analysed during this study are included in this published article. This manuscript has associated data in a data repository. [Authors' comment: All data generated or analysed during this study are included in this published article: <https://doi.org/10.1140/epjp/s13360-023-04222-8>.]

**Open Access** This article is licensed under a Creative Commons Attribution 4.0 International License, which permits use, sharing, adaptation, distribution and reproduction in any medium or format, as long as you give appropriate credit to the original author(s) and the source, provide a link to the Creative Commons licence, and indicate if changes were made. The images or other third party material in this article are included in the article's Creative Commons licence, unless indicated otherwise in a credit line to the material. If material is not included in the article's Creative Commons licence and your intended use is not permitted by statutory regulation or exceeds the permitted use, you will need to obtain permission directly from the copyright holder. To view a copy of this licence, visit <http://creativecommons.org/licenses/by/4.0/>.

## References

1. L. Giacomelli, A. Perrotta, R. Scandone, C. Scarpati, *Episodes* **26**, 235 (2003)
2. N. Prieto-Taboada, S. Fdez-Ortiz de Vallejuelo, A. Santos, M. Veneranda, K. Castro, M. Maguregui, H. Morillas, G. Arana, A. Martellone, B. de Nigris, M. Osanna, J.M. Madariaga, *J. Raman Spectrosc.* **52**(1), 85–94 (2020)
3. M. Veneranda, N. Prieto-Taboada, S. Fdez-Ortiz de Vallejuelo, M. Maguregui, H. Morillas, I. Marcaida, K. Castro, F.J. Garcia-Diego, M. Osanna, J.M. Madariaga, *Spectrochim. Acta Part A Mol. Biomol. Spectrosc.* **203**, 201 (2018)
4. I. Marcaida, M. Maguregui, H. Morillas, N. Prieto-Taboada, M. Veneranda, S. Fdez-Ortiz de Vallejuelo, A. Martellone, B. De Nigris, M. Osanna, J.M. Madariaga, *Herit. Sci.* **7**, 1 (2019)
5. P. Ricciardi, P. Colombaro, A. Tournié, M. Macchiarola, N. Ayed, *J. Archaeol. Sci.* **36**, 2551 (2009)
6. M. Veneranda, S. Fdez-Ortiz de Vallejuelo, N. Prieto-Taboada, M. Maguregui, I. Marcaida, H. Morillas, A. Martellone, B. de Nigris, M. Osanna, K. Castro, J.M. Madariaga, *Herit. Sci.* **6**, 1 (2018)
7. O. Williams-Thorpe, *Archaeometry* **37**, 217 (1995)
8. R.H. Tykot, *J. Mediterr. Archaeol.* **9**, 39 (1996)
9. R.G.V. Hancock, T. Carter, *J. Archaeol. Sci.* **37**, 243 (2010)
10. L. Bellot-Gurlet, G. Poupeau, J. Salomon, T. Calligaro, B. Moignard, J.C. Dran, J.A. Barrat, L. Pichon, *Nucl. Inst. Methods Phys. Res. Sect. B Beam Interact. Mater. Atoms.* **240**(1–2), 583–588 (2005)
11. S.C. Lynch, A.J. Locock, M.J.M. Duke, A.W. Weber, *J. Radioanal. Nucl. Chem.* **309**, 257 (2016)
12. F. Italiano, A. Correale, M. Di Bella, F.F. Martin, M.C. Martinelli, G. Sabatino, F. Spatafora, *Mediterr. Archaeol. Archaeom.* **18**, 151 (2018)
13. M. Orange, F.X. Le Bourdonnec, A. Scheffers, R. Joannes-Boyau, *Sci. Technol. Archaeol. Res.* **2**, 192 (2016)
14. R. Bugoi, B. Constantinescu, C. Neelmeijer, F. Constantin, *Nucl. Instrum. Methods Phys. Res. Sect. B Beam Interact. Mater. Atoms.* **226**(1–2), 136–146 (2004)
15. D. Barca, G. Lucarini, F.G. Fedele, *Archaeometry* **54**, 603 (2012)
16. D.D. Rindel, S.I. Perez, R. Barberena, B.L. MacDonald, M.D. Glascock, *Archaeometry* **62**, 1 (2020)
17. A.M. De Francesco, G.M. Crisci, M. Bocci, *Archaeometry* **50**, 337 (2008)
18. A. Anguissola, S. Legnaioli, E. Odelli, V. Palleschi, S. Raneri, *Marmora Int. J. Archaeol. Hist. Archaeom. Marbles Stone* **17**, 67 (2021)
19. A. McAlister, *Archaeol. Ocean.* **54**, 131 (2019)
20. E. Frahm, R. Doonan, V. Kilikoglou, *Archaeometry* **56**, 228 (2014)
21. Z. Kasztovszky, B. Maróti, I. Harsányi, D. Párkányi, V. Szilágyi, *Quat. Int.* **468**, 179 (2018)
22. M. Veneranda, N. Prieto-Taboada, I. Costantini, A.M. De Francesco, K. Castro, J.M. Madariaga, and G. Arana, *Anal. Chem.* Under review (2021)
23. S.M. Zaytsev, I.N. Krylov, A.M. Popov, N.B. Zorov, T.A. Labutin, *Spectrochim. Acta Part B At. Spectrosc.* **140**, 65 (2018)
24. V. Lazic, M. Vadrucchi, R. Fantoni, M. Chiari, A. Mazzinghi, A. Gorghinian, *Spectrochim. Acta Part B At. Spectrosc.* **149**, 1 (2018)
25. C. García-florentino, M. Maguregui, H. Morillas, I. Marcaida, J. Manuel, *Microchem. J.* **133**, 104 (2017)
26. L.H. Petersen, *Arethusa* **45**, 319 (2012)
27. G. Bigazzi, F.P. Bonadonna, *Nature* **242**, 322 (1973)
28. R.H. Tykot, T. Setzer, M.D. Glascock, R.J. Speakman, *Geoarchaeol. Bioarchaeol. Stud.* **3**, 107 (2005)

29. V. Francaviglia, J. Archaeol. Sci. **15**, 109 (1988)
30. R.H. Tykot, J. Archaeol. Sci. **24**, 467 (1997)
31. D. Syvilay, B. Bousquet, R. Chapoulie, M. Orange, F.X. Le Bourdonnec, J. Anal. At. Spectrom. **34**, 867 (2019)
32. J.J. Remus, J.L. Gottfried, R.S. Harmon, A. Draucker, D. Baron, R. Yohe, Appl. Opt. **49**, 1990 (2010)
33. I. Liritzis and N. Zacharias, in *X-Ray Fluoresc. Spectrom. Geoarchaeology*, edited by M. S. Shackley (Springer New York, New York, NY, 2011), pp. 109–142.
34. C. Huffman, H. Sobral, E. Terán-Hinojosa, Spectrochim. Acta Part B Atom. Spectros. **162**, 105721 (2019)
35. V. Renda, V. Mollica Nardo, G. Anastasio, E. Caponetti, C.S. Vasi, M.L. Saladino, F. Armetta, S. Trusso, R.C. Ponterio, Spectrochim Acta Part B At. Spectrosc. **159**, 105655 (2019)
36. Y. Ralchenko, A. Kramida, Atoms **8**, 1 (2020)
37. M. Veneranda, J. Saiz, G. Lopez-reyes, J. A. Manrique, A. Sanz, C. Garcia-prieto, S. C. Werner, A. Moral, J. M. Madariaga, and F. Rull, in *Eur. Sci. Congr. (Virtual, 2020)*.
38. A.A.E. Fisher, J. Chem. Educ. **96**, 1502 (2019)
39. S.Y. Krotova, A.E. Ilin, A.V. Chirgin, Int. J. Mech. Eng. Technol. **10**, 1823 (2019)
40. J. Kawai, K. Yamasaki, and R. Tanaka, Encycl. Anal. Chem. **1** (2019).
41. R.H. Tykot, Acc. Chem. Res. **35**, 618 (2002)
42. D. Barca, A.M. De Francesco, G.M. Crisci, J. Cult. Herit. **8**, 141 (2007)
43. M. Orange, F.X. Le Bourdonnec, L. Bellot-Gurlet, C. Lugliè, S. Dubernet, C. Bressy-Leandri, A. Scheffers, R. Joannes-Boyau, J. Archaeol. Sci. Reports **12**, 834 (2017)
44. M. Milić, J. Archaeol. Sci. **41**, 285 (2014)
45. F.K. Nadooshan, A. Abedi, M.D. Glascock, N. Eskandari, M. Khazaei, J. Archaeol. Sci. **40**(4), 1956–1965 (2013)
46. Y.V. Kuzmin, C. Oppenheimer, C. Renfrew, Quat. Int. **542**, 41 (2020)
47. B. Gratuze, J. Archaeol. Sci. **26**, 869 (1999)
48. A.M. De Francesco, A. La Marca, C. Colelli, D. Barca, Minerals **12**, 1 (2022)
49. S. Cagno, P. Cosyns, A. Izmer, F. Vanhaecke, K. Nys, K. Janssens, J. Archaeol. Sci. **42**, 128 (2014)
50. I. van der Werf, A. Mangone, L.C. Giannossa, A. Traini, R. Laviano, A. Corolini, L. Sabbatini, J. Archaeol. Sci. **36**, 2625 (2009)
51. C. Boschetti, J. Henderson, J. Evans, J. Archaeol. Sci. Reports **11**, 647 (2017)
52. E. Basso, C. Invernizzi, M. Malagodi, M.F. La Russa, D. Bersani, P.P. Lottici, J. Raman Spectrosc. **45**, 238 (2014)
53. P. Cosyns, S. Cagno, K. Janssens, K. Nys, Integr. Approach. Study Hist. Glas. **8422**, 842203 (2012)
54. P. Degryse, *Glass Making in the Greco-Roman World*, 1st edn. (Leuven University Press, Leuven, 2014)
55. I.C. Freestone, K.A. Leslie, M. Thirlwall, Y. Gorin-Rosen, Archaeometry **45**, 19 (2003)
56. D. Brems, M. Ganio, K. Latruwe, L. Balcaen, M. Carremans, D. Gimeno, A. Silvestri, F. Vanhaecke, P. Muechez, P. Degryse, Archaeometry **55**, 214 (2013)
57. I.C. Freestone, Mater. Res. Soc. Symp. Proc. **852**, 195 (2005)